A Practical and Inexpensive System for Natural Gas Leak Remote Detection

Bo Ling, Michael Zeifman, Jason Hu
Migma Systems, Inc.
1600 Providence Highway
Walpole, MA 02081
(*bling, mzeifman, jhu@migmasys.com*)

Abstract

Detecting gas leaks is difficult. Gas emerges from pipelines with no warning and is blown downwind, rapidly diluting as it moves forward. Traditional point sampling detectors are therefore limited to detecting leaks at a short distance away, which means that permanently installed sensors must be carefully sited, and hand-held sensors are time-consuming to use. In this paper, a new approach for the gas leak detection is introduced*. In this system, the sunlight is utilized as the light source for methane detection, which makes the system a viable choice of commercial gas leak remote detection applications. The spectral absorbance in the wave range of 850-950 nm is used in this system for the absorbance decomposition based on Independent Component Analysis. Hilbert Transform based shape analysis is applied to the decomposed spectral absorbance for methane detection and classification. The actual field tests have shown that this system can indeed detect the methane in a very low concentration.

Keywords: gas leak detection, ICA (Independent Component Analysis), Hilbert transform, feature extraction, classification, NIR spectra.

I. Introduction

America receives over two-thirds of the crude and petroleum products for more than 55 million residential and commercial customers, through more than 160,000 miles of pipelines. In addition, over 326,000 miles of gas transmission pipelines transport natural gas to local companies that distribute it to local customers. This supply of energy has too often been disrupted by local pipeline leaks.

Detecting gas leaks is difficult. Gas emerges from pipelines with no warning and is blown downwind, rapidly diluting as it moves forward. Traditional point sampling detectors are therefore limited to detecting leaks at a short distance away, which means that permanently installed sensors must be carefully sited, and hand-held sensors are time-consuming to use. A low parts per million (ppm) gas concentration might be an indication of higher, explosive or toxic concentrations closer to the leak or of a developing situation. Single point sampling is inefficient, and gives little information about the relative scale of the leak.

Imaging gas leaks has long been thought a potential solution to remote gas leak detection: a wide area could be scanned rapidly from a remote position, the image would convey both the location of the leak source and the wind direction, and complicated multi-source leaks would be easier to interpret. There are two alternatives for such remote sensing techniques:

*** Methods presented here are protected by Migma's US Provisional Patent.**

(1) active detection, which requires illuminating the scene with a radiation source, usually a laser, that is absorbed by the target gas, and
(2) passive detection (also called thermal detection), which relies on radiative transfer due to a temperature and/or emissivity difference that usually exists between the background and the target methane (CH_4) plume.

While passive methods allow nearly unlimited range with a simple instrumental configuration, these methods rely upon a thermal flux between the gas plume and the ground surface below it. Active detection removes the thermal constraint, but requires a laser and a scattering surface behind the gas for generation of the signal.

Because passive methods require a temperature/emissivity difference with the background, the detected gas will appear invisible at the temperature for which there is no net radiative heat transfer between the gas and the surroundings. Several schemes have been considered for passive methods to enhance the detection of natural gas (Hodgkinson 2005). The surface changes of the ratio of scattering to the sum of absorption and scattering can be misinterpreted as temperature differences, resulting in false positive readings. The existing passive imaging methods all suffer one major problem: gas plume can be too light in the image to be detected. It has been reported (Hodgkinson 2005) that the gas leaks of 1 liter/min could only be detected in light winds with ΔT in the range of 1ºC to 5ºC, but the best quality images were recorded using a high ΔT of 30ºC.

Since the existing active detection system is too expensive and passive detection system is less reliable, a system has been developed at Migma, which utilizes *sunlight* during daytime to detect the methane, a major component in natural gas, within 850-950 nm wavelength range. Being able to detect the methane within this range is significant, which makes it possible to dramatically reduce the system cost associated with an expensive NIR spectrometer, an expensive laser device, and complex and costly system operations. This system utilizes Migma's patented technology to reliably calculate the spectral absorbance during different time of a day under various weather conditions. This is achieved by applying a pattern matching technique using a set of normalized light intensity profiles estimated from the vacuum scanning.

Since the spectral absorbance within 850-950 nm wavelength range is primarily dominated by the water vapor in the air, the ICA (Independent Component Analysis) method has been used to decompose the spectral absorbance signal into a set of independent spectral signals representing the species present in the air, which include H_2O, O_2, and CH_4 in the case of gas leak. The independent component analysis (ICA) is a newly developed statistical approach to separating unobserved, independent source variables from the observed variables that are the combinations (or mixtures) of these source variables. Since it was developed in the 1990s (Comon, 1994; Hyvarinen, 1999; Jutten and Herault, 1991), ICA has proved to be a successful technique in biomedical signal processing (Vigario, 1997), magnetic resonance imaging analysis (Biswal and Ulmer, 1999), speech recognition (Park et al, 1999) and machine monitoring (Ypma and Pjunen, 1999).

To detect and classify methane from these unmixed spectral absorbance signals, the shapes of decomposed signals are compared with the theoretical methane shape by utilizing Hilbert Transform (Hahn 1996). HT has been widely used for signal envelop extraction (Long 1995). It has been found that the shapes of the theoretical and decomposed methane signals in different wave bands are quite similar. Therefore, instead of matching the spectral peaks, the system presented here extracts the envelops of the theoretical methane absorbance and the decomposed methane absorbance for the methane detection and classification.

This paper is organized as follows: In Section II, Migma's patented technologies, used to calculate the methane spectral absorbance for different time of a day under any weather conditions, are briefly described. In Section III, the ICA method is intrduced, which overcomes various shortcomings of traditional ICA methodologies. The gas leak detection method is described in Section IV where Hilbert Transform based shape matching approach is given. The detection sensitivity estimation results are shown in Section V.

II. Methane Spectral Absorbance Calculation

Beer-Lambert's law governs the estimation of methane's spectral absorbance. It specifies the linear relationship between the absorbance and concentration of absorbing species, including methane to be detected in the outdoor open air. The general Beer-Lambert's law is usually given as:

$$A_\lambda = \varepsilon_\lambda bc \tag{2.1}$$

where A_λ is the absorbance, ε_λ is the absorptivity coefficient at wavelength λ, b is the path length of the species (such as methane, CH_4), c is the concentration of the same species. It can be observed that absorbance is proportional to both path length and methane concentration. The theoretical absorbance of methane used in this system is taken from the published data (O'Brien 2002). Figure 2-1 shows the methane absorbance with path length of 100 meters and concentration being 1000 ppm.

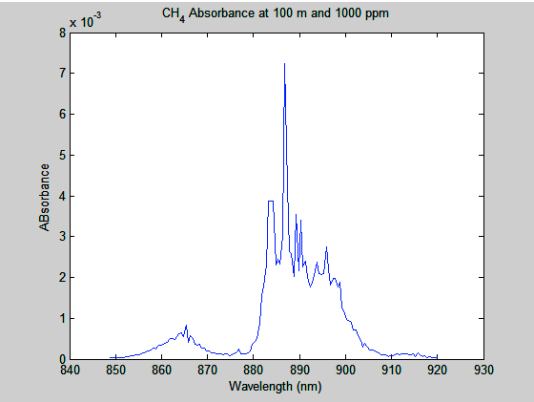

Figure 2-1: Methane absorbance at 100m path length and 1000ppm concentration over wavelength range of 850 – 920nm.

Since the NIR spectrometer used in Migma's gas leak detection system has the wavelength range of 500-1200nm, to detect the methane, the sub-range of 850-950nm is mainly used. Compared to the expensive IR spectrometers which can detect the methane at higher wavelength ranges, the challenging issues working in the range of 850-950nm is that methane does not have distinctive peaks. In fact, the absorbance in this wavelength region is mainly dominated by water vapor (H_2O). Another common specie in this region is oxygen (O_2). In next section will detail the absorbance decomposition scheme using ICA (Independent Component Analysis).

To obtain the absorbance from the spectrometer, it is necessary to first take the "dark" scan and "vacuum" scan. Basically, the "dark" scan will measure the light intensity in a totally dark environment while the "vacuum" scan is done in a *vacuum* environment. Mathematically, the absorbance at pixel n can be calculated using the following formula:

$$A_n = -\log\left(\frac{s_n - d_n}{v_n - d_n}\right) \qquad n = 1, 2, \ldots, N \tag{2.2}$$

where N is the number of pixels supported by the spectrometer, s_n is the real-time light intensity measurement from the spectrometer, v_n is the light intensity measurement in the vacuum environment, and d_n is the light intensity measured in a totally dark environment. Therefore, in order to have an accurate absorbance, one must

measure the light intensity in both "dark" and "vacuum" environment. Since d_n is close to zero, Eq. (2.2) can be further simplified as

$$A_n = -\log\left(\frac{s_n}{v_n}\right) \qquad n = 1, 2, ..., N \tag{2.3}$$

which has been used in the system for the methane absorbance calculation. The value of A_n is always non-negative since $v_n \geq s_n$ for $n = 1, 2, \ldots, N$.

One important assumption in using Eq. (2.3) for the absorbance calculation is that both s_n and v_n are measured under the same lighting condition, i.e., light intensity from the light source must remain the same. For the methane detection using sunlight, this assumption is extremely difficult to satisfy for the following reasons:

(1) sunlight intensity strongly depends on the time and weather condition of a day.
(2) vacuum reference is almost impossible to collect in the outdoor changing environment.

The system reported here utilizes Migma's patented technologies to overcome these challenges. Since the spectral absorbance characterizes the absorption of a specie, it is independent of the incident light used in the measurement. The solar radiation is taken as solar reference, and the corresponding reference is taken in the lab, which is close to the solar reference. Under the same settings, light source reference is taken and Eq. (2.3) is used to calculate the absorbance by utilizing solar radiation measurement and light source reference from the library. Since this system is operating in near real time, solar radiation will be observed continuously.

More specifically, let's assume that the actual sunlight photon counts curve is $s_n \equiv s_s(\lambda)$, the matching reference photon counts curve is $s(\lambda)$ and the corresponding vacuum reference is $v_n \equiv v(\lambda)$. The references are obtained from a measuring device with length of b_1 = 10 m. Let the generally unknown path length of the sunlight be b_s. Then, if the air compositions are the same, one can, using Eq. (2.3), re-write Eq. (2.1) in the following forms for the measuring device and for the open air:

$$\log\frac{v(\lambda)}{s(\lambda)} = \varepsilon(\lambda)cb_1 \tag{2.4}$$

$$\log\frac{v_s(\lambda)}{s_s(\lambda)} = \varepsilon(\lambda)cb_s \tag{2.5}$$

From these equations, the sought vacuum reference for the sunlight can be estimated from

$$\frac{v_s(\lambda)}{s_s(\lambda)} = \left(\frac{v(\lambda)}{s(\lambda)}\right)^{\frac{b_s}{b_1}} \tag{2.6}$$

Suppose that some methane is now present in the open air so that the photon counts curve of sunlight will be modified to $s_{s,m}(\lambda)$. Accordingly, the "true absorbance" Eq. (2.5) will be modified as follows:

$$A_t = \log\frac{v_s(\lambda)}{s_{s,m}(\lambda)} = [\varepsilon(\lambda)c + \varepsilon_m(\lambda)c_m]b_s \tag{2.7}$$

Using Eq. (2.6), it follows that:

$$A_t = \log\frac{s_s(\lambda)}{s_{s,m}(\lambda)} + \frac{b_s}{b_1}\log\frac{v(\lambda)}{s(\lambda)} = [\varepsilon(\lambda)c + \varepsilon_m(\lambda)c_m]b_s \tag{2.8}$$

Let's analyze what happens if $v_s(\lambda) = v(\lambda)$. This is equivalent to setting $b_s = b_1$ in Eq. (2.8) provided that $s_s(\lambda) = s(\lambda)$, so that approximate absorbance A_a will be given by

$$A_a = \log\frac{s_s(\lambda)}{s_{s,m}(\lambda)} + \log\frac{v(\lambda)}{s(\lambda)} \tag{2.9}$$

It follows from Eqs. (2.8)-(2.9) that

$$A_a = [\varepsilon(\lambda)c + \varepsilon_m(\lambda)c_m]b_s + \left(\frac{b_s}{b_1} - 1\right)\log\frac{v(\lambda)}{s(\lambda)} \tag{2.10}$$

The logarithm in Eq. (2.10) is simply the spectrum of air obtained in laboratory. Therefore, Eq. (2.10) can be further re-written as

$$A_a = \varepsilon(\lambda)c(2b_s - b_1) + \varepsilon_m(\lambda)c_m b_s \tag{2.11}$$

For the conventional spectroscopy methods, it is necessary to know the effective sunlight path b_s that enters Eq. (2.11). In the method based on the ICA decomposition, it is not necessary to know this value so that Eq. (2.11) constitutes a basis for the proposed use of the laboratory vacuum references. Note that in virtue of Eq. (2.11), the methane contribution to the total approximate absorbance signal is not distorted as is, for example, in the differential optical absorption spectroscopy (DOAS) which is commonly used in the open air spectroscopy (Platt, 1994).

However, since the number of references in the library is limited, one must consider the uncertainties associated with references matching. The absorbance variation is define as

$$\Delta A = A_{SR} - A_S \tag{2.12}$$

where A_{SR} is the absorbance calculated based on the solar radiation and reference measured in the vacuum environment, and A_S is the absorbance calculated using the solar radiation and reference matched from the reference library. Using Beer-Lambert's law, it can be easily verified that

$$s = s_r \times 10^{\Delta A} \tag{2.13}$$

where s is the measured solar radiation and s_r is corresponding vacuum reference. Since the light intensity range is known *a priori*, the spectral intervals are formed by dividing the entire range into a set of intervals. The number of spectral intervals is chosen such that the uncertainty associated with each interval is within the desired level. In this way, if a measured solar radiation falls in one particular interval, its related vacuum reference can be chosen from the reference library, which in turn makes it possible for the calculation of absorbance in any outdoor conditions.

III. Absorbance Decomposition via ICA

Let **X** be a column matrix of mixed signals. The goal is to decompose **X** into a set of signals. Using the standard ICA methodology, one can write

$$\mathbf{X} = \mathbf{A} \cdot \mathbf{S} \tag{3.1}$$

where **A** is a matrix representing the signal abundance and **S** is the column matrix of the source signals. With relation to the spectroscopic signals (viz. spectra), Eq. (3.1) represents both Beer-Lambert's law and the principle of superposition. Indeed, a column of **X** is given by

$$\mathbf{X}_i(\lambda) = \mathbf{A}_{11} \times \mathbf{S}_{i1}(\lambda) + \mathbf{A}_{12} \times \mathbf{S}_{i2}(\lambda) + \ldots \tag{3.2}$$

The Beer-Lambert law implies that $\mathbf{A}_{ij}$ are wavelength-independent constants and the linear summation implies the superposition principle. Because of the linearity of Eq. (3.1), the inverse equation is also linear:

$$\mathbf{S} = \mathbf{A}^{-1} \cdot \mathbf{X} = \mathbf{B} \cdot \mathbf{X} \tag{3.3}$$

The key idea of ICA method is that thanks to the Central Limit Theorem, a weighted sum of column vectors of **X** in (Eq. 3.3) approaches to a normal distribution unless it accidentally equals to one of vectors of matrix **S**. Therefore, by multiplying different matrices by the signal matrix and by measuring the degree of Gaussianity of their product, the independent components can be detected. Of course, this formulation can only help finding the "form" of the independent components, as scaling the matrix **B** will also scale the solution, while the degree of non-Gaussianity would not change.

ICA usually starts from a pre-procedure of "whitening". The key idea here is that if the signals are independent, then they are uncorrelated, which in turn means that a procedure that decorrelates matrix **X** is a necessary (but not sufficient) procedure for estimating the independent signals. The two-stage procedure will be maximally efficient if one also requires unit variances of the decorrelated components, because, in this case, the meaning of the matrix **B** will be pure rotation of the "whitened" matrix **X**. That is, ICA is usually performed in two stages:

1) $\mathbf{Z} = \mathbf{\Omega X}$
2) $\mathbf{W}: \quad \mathbf{W} \cdot \mathbf{Z} \rightarrow \max(non - Gauss)$

The matrix **W** in this case is an orthonormal matrix which can be considered as a rotation matrix in the *n*-dimensional space. Various degrees of non-Gausianity have been proposed so far, for example an estimated kurtosis or entropy can be used. Since for a normal distribution both kurtosis and the negative entropy are minimal possible among all possible distributions for the whitened signals, their maximization will yield maximum of non-Gaussianity. As for the first transform, it is just a well-known transform in principal component analysis (PCA) so that the matrix $\mathbf{\Omega}$ can be easily calculated on the basis of covariance matrix of **X**.

The necessity for the two-stage procedure in ICA demonstrates the inherent ICA limitations. Actually, they are the same as in PCA, and, with application to our spectral absorbance unmixing problem, these limitations are

- The number of independent components can only be decided on the basis of the analysis of the signal covariance matrix (its eigenvalues)
- Trace components may not be recovered if the noise is present
- The components can be recovered up to a scaling factor, i.e., scaling the solution does not change ICA.

The second limitation is originated from the fact that PCA decorrelates variables on the basis of their contribution to the overall variance. An additional limitation of a traditional ICA is that it is not sensitive to the order of variables comprising a mixture vector. In other words, a random permutation of the obtained spectrum will not influence the conventional ICA in any way. These limitations call for the development of more advanced algorithms for spectral absorbance unmixing.

To decompose signals in time series, the temporal ICA can also be applied. The key idea behind temporal ICA is to exploit the internal structure of the mixed signals. The simplest form of time structure is given by autocovariances. This means the covariances between the values of the signal at different waveband points: cov $[\mathbf{x}_i(\lambda), \mathbf{x}_i(\lambda-\Delta)]$, where Δ is the waveband lag. The value of $\Delta = 1$ corresponds to the covariance between two adjacent points in the spectrum.

In addition to the covariances of one spectrum, we also need covariances between two signals: cov $[\mathbf{x}_i(\lambda), \mathbf{x}_j(\lambda-\Delta)]$. These statistics can be combined in the lagged covariance matrix

$$\mathbf{C}_{\Delta}^{x} = E[\mathbf{x}(\lambda)\mathbf{x}(\lambda-\Delta)^{T}]. \tag{3.4}$$

In Eq. (3.4) E designates the statistical expectation. Now, for the independent components, the lagged covariances matrix is a diagonal matrix because of their independence. We should, therefore, seek for such matrix **B** that the lagged covariance matrix of $\mathbf{Y} = \mathbf{BX}$ is diagonal.

Let us assume that the data matrix **X** has been whitened so that the resulting matrix **Z** contains non-correlated vectors (spectra) with unit variances. Since the lagged covariance matrix in Eq. (3.4) is estimated by the experimental data, the matrix may not be exactly symmetric (the delay to the left may slightly differ from the delay to the right), although the true matrix is symmetric. To remedy this problem we consider

$$\overline{\mathbf{C}}_{\Delta}^{z} = \frac{1}{2}[\mathbf{C}_{\Delta}^{z} + (\mathbf{C}_{\Delta}^{z})^{T}] \tag{3.5}$$

Suppose **W** is the matrix we are looking for, i.e., that $\mathbf{S} = \mathbf{WZ}$. Then, it follows from Eqs. (3.4) – (3.5) that

$$\overline{\mathbf{C}}_{\Delta}^{z} = \frac{1}{2}\mathbf{W}^{T}\left\{E[\mathbf{s}(\lambda)\mathbf{s}(\lambda-\Delta)^{T}] + E[\mathbf{s}(\lambda-\Delta)\mathbf{s}(\lambda)^{T}]\right\}\mathbf{W} = \mathbf{W}^{T}\overline{\mathbf{C}}_{\Delta}^{s}\mathbf{W} \tag{3.6}$$

Because of the source independence, the matrix $\overline{\mathbf{C}}_{\Delta}^{s}$ is diagonal. This means that the required matrix **W** is part of the eigenvalue decomposition of the estimable matrix $\overline{\mathbf{C}}_{\Delta}^{z}$. Since we enforced this matrix to be symmetric, its eigenvalue decomposition is simple to compute. In addition, there is no necessity to calculate the components in a sequence, i.e., "deflationally" – all components will be calculated simultaneously.

The "temporal" two-stage procedure works as follows:

1) Whiten the matrix of obtained spectra using PCA techniques (e.g., using the eigenvalue decomposition of the covariance matrix). Decide the number of components.
2) Compute the eigenvalue decomposition of lagged covariance matrix, Eq. (3.5).
3) The required matrix **W** comprises eigenvectors of the lagged matrix.

As we can see, there is no need for the non-Gaussianity maximization or for any iterative optimization algorithm. The algorithm is extremely fast and reliable. However, because most of the source spectra are sparse,

the algorithm may not work always properly. In order to overcome the major drawbacks of temporal ICA, we have developed a combined temporal – conventional algorithm for ICA. The algorithm first processes temporal ICA. The value of the calculated "rotational" matrix **W** is then used for "fine tuning" realized by a conventional ICA. We use the negative entropy (negentropy) as the measure of non-Gaussianity and utilize a fast converging gradient optimization algorithm.

IV. Natural Gas Leak Detection Using Sunlight as Light Source

As stated in Section II, the spectral absorbance calculated in the wavelength of 850-950 nm is dominated by the water vapor (H_2O). Figure 4-1 shows an example of absorbance obtained outdoor during a sunny day. From the theoretical methane absorbance shown in Figure 2-1, there is a large peak at 877 nm. However, this peak is hardly seen in Figure 4-1. Therefore, the traditional spectral peak detection methods are no longer effective, which partially explains why sunlight has not been widely used for the methane detection except for the passive thermal detection systems.

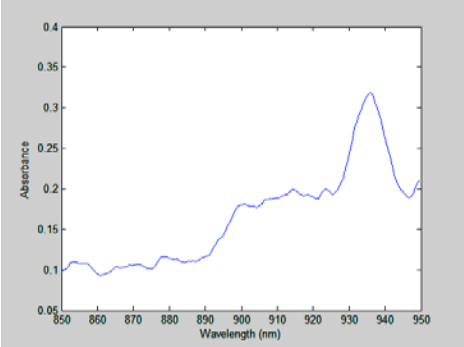

Figure E.4-1: An example of outdoor open air spectral absorbance.

To extract methane from the open air spectral absorbance in 850 – 950 nm wave band, ICA method has been applied in the system. ICA can effectively decompose mixed signals which are statistically independent and non-Gaussian distributed. The statistical independence required by ICA is a stronger condition than the statistical uncorrelatedness required by the PCA. Seeking independent rather than uncorrelated features exploits more information hidden in the higher order statistics, and leads to uniquely identified source components. Figure 4-2(a) shows an example of an open air absorbance collected at a place where the gas leak was observed. Figure 4-2(b) shows the ICA decomposed methane (bottom) which closely resembles the theoretical methane absorbance (top) both in peak location and shape.

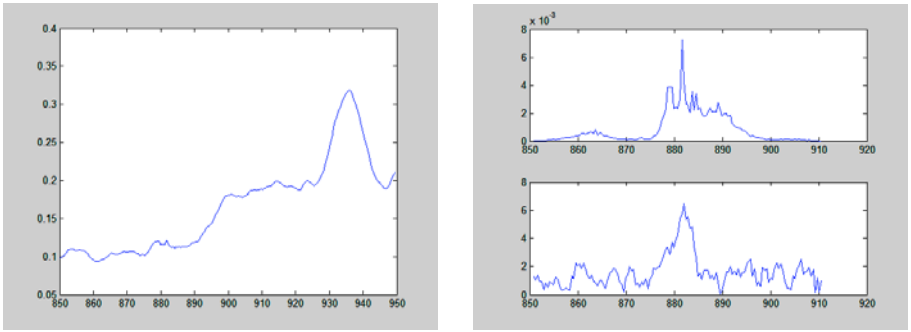

(a) (b)

Figure 4-2: (a) Open air spectral absorbance with methane present. (b) Theoretical (top) and decomposed (bottom) methane absorbance.

Sine ICA tends to smooth the signals, signals with large variations such as methane may not be decomposed accurately. Therefore, one can select sub-bands and decompose the signals accordingly. Figure 4-3 shows the decomposed methane in wave band of 875 – 906 nm and 850 – 876 nm where methane shows strong signals. In both cases, the decomposed methane absorbance is very similar to the theoretical methane absorbance in the corresponding wave bands.

In general, ICA generates a set of decomposed signals. The actual number of true mixed signals is difficult to estimate. In practice, one can choose a large number such as 20 and obtain 20 decomposed signals. The next step is to classify among these decomposed signals to determine whether or not the methane is actually present.

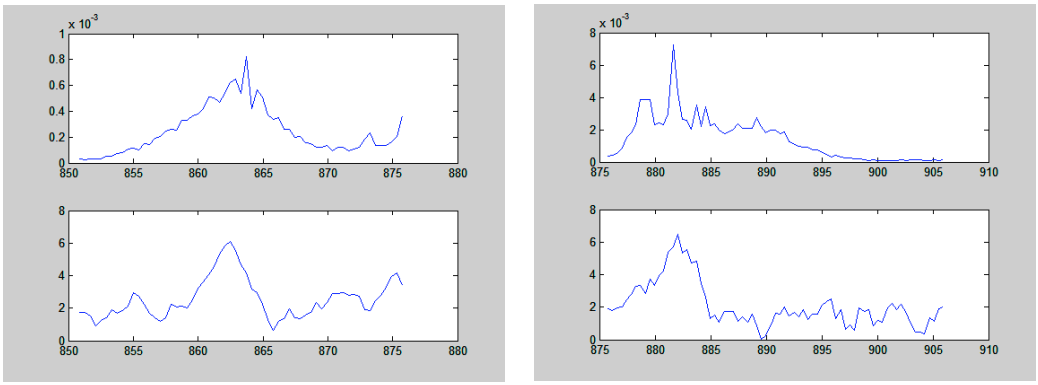

(a) (b)

Figure 4-3: (a) Theoretical (top) and decomposed (bottom) methane absorbance in wave band of 850 – 876 nm. (b) Theoretical (top) and decomposed (bottom)methane absorbance in wave band of 876 – 906 nm.

From Figure 4-3, it can be observed that the shapes of the theoretical and decomposed methane signals in different wave bands are quite similar. Therefore, instead of matching the signals based on peak locations which might shift, our system extracts the envelops of the theoretical methane absorbance and the decomposed methane absorbance. A common and very efficient technique for the envelope detection is based on the Hilbert Transform.

The Hilbert Transform of $f(t)$ is defined as

$$H[f] = \tilde{f}(x) = \frac{1}{\pi}\int_{-\infty}^{\infty}\frac{f(t)}{t-x}dt \qquad (4\text{-}1)$$

where the integral is a Cauchy principal value. In particular, the complex signal defined as

$$z(t) = f(t) + i\cdot\tilde{f}(t) \qquad (4\text{-}2)$$

is an analytic signal which does not have the negative-frequency components. The amplitude of the complex signal, $|z(t)|$, represents the envelope of the signal $f(t)$. In the system, Hilbert Transform to detect the presence of methane.

V. System Sensitivity Estimation

An important parameter that defines the sensitivity of the gas leak detection system is the product of gas concentration and the optical path length. In the open air experiments, the concentration of methane is not constant in time and space so that direct measurement of the sensitivity is difficult. We have, therefore, designed special experiments to measure the sensitivity of our system, GasTutamen™.

In these experiments, we measure the absorbance spectrum of a gas trapped within a small plastic tube. If the tube is connected to a gas cylinder, the gas will flow inside the tube. Provided that the gas flow velocity is low, the gas pressure inside the tube will be approximately equal to the atmospheric ambient pressure, while the equivalent optical path length can be easily calculated. Such experiments can be benchmarked with the experiments in which no methane flow is supplied to the tube, in order to assess the false positives.

Figure 5-1 shows a photograph of our experimental system. The spectrometer is mounted on a tripod and connected to a power source and to a laptop computer. The gas cylinder contains a 2.5 ± 0.05 % methane mixture with nitrogen. A transparent plastic tube is connected to the gas cylinder and comes across the spectrometer's field of view. The free end of the tube is covered with a punctured plastic tape, in order to preserve weak but nonzero gas flow through the tube.

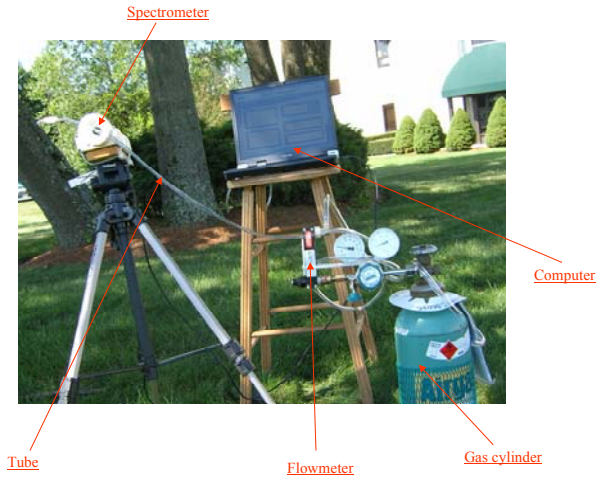

Figure 5-1: Experimental system for measurement of gas detection sensitivity.

Once the gas vent is open, the gas flow through the tube can be maintained with the flowmeter. Fig. 5-2 shows the data acquisition part of the system. The flowmeter is set to 8 standard cubic feet per hour (scf/h) flow rate. The gas flows through the tube, which is fixed in a custom-made fixture. In this way, the light, entering the spectrometer through an IR filter, will penetrate the tube.

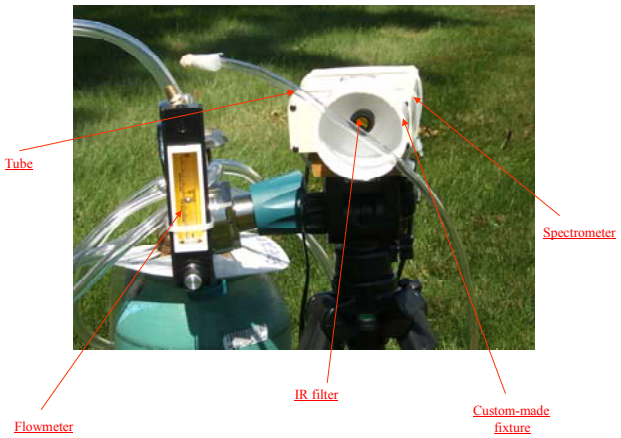

Figure 5-2: Data acquisition part of the experimental system. The gas flow is set to 8 scf/h.

The internal diameter of the tube is 5 mm which is less than the IR filter/spectrometer slit diameters (see Figure 5-3), so that the equivalent optical path length is given by

$$\overline{L} = \frac{\int_0^R 2\sqrt{R^2 - x^2}\,dx}{R} = \frac{\pi R}{2} \approx 3.93 \text{ (mm)} \qquad (5\text{-}1)$$

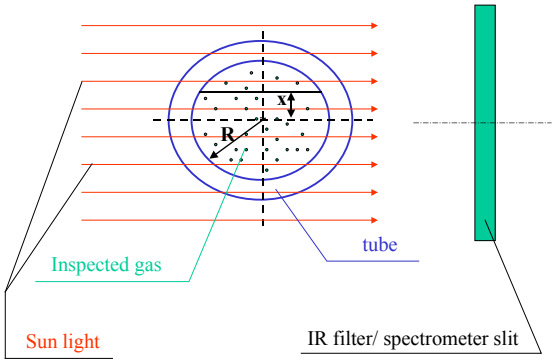

Figure 5-3: A cross section of the data acquisition system.

The concentration of 2.5% of methane inside the tube is 25 000 ppm. If the presence of methane can be detected by the described experimental system, the system sensitivity is or better than

$$25000 \times 0.00393 = 98.25 \text{ (ppm} \cdot \text{m)}. \qquad (5\text{-}2)$$

This sensitivity is good as compared with the sensitivity of similar but much more expensive experimental systems. The actual sensitivity of our system can be even better than the one specified by eq. (5-2). There are two factors that decrease the sensitivity of the experimental system described above. First, the tube diameter is less than the diameter of the IR filter/ spectrometer slit so that the total light entering the spectrometer is a mixture of a sun light and the tube-absorbed light. Second, the plastic tube may reflect and absorb light, too, thus decreasing the quality of the gas absorbance spectrum.

The actual detection results of the field experiments for the system shown in Figs. 5-1 – 5-2 are depicted in Fig. 5-4. For the benchmarking, we used a free tube identical to the one used for the methane flow experiments. The reason for using a separate tube is that some methane may be trapped inside the tube and cause methane detection even if the tube is no longer connected to the gas cylinder.

VI. Conclusion

In this paper, we have presented an innovative system for remote gas leak detection by utilizing sunlight as the light source. The spectral absorbance in the wave range of 850-950 nm is used for signal decomposition based on the independent component analysis. Hilbert Transform based shape analysis is applied to the decomposed spectral absorbance for methane detection and classification. Actual field tests have shown that our system can detect methane in a very low concentration. Because we avoid using the expensive laser light source and expensive spectrometer, our system is a viable choice of commercial gas leak remote detection applications..

Acknowledgement: This work is supported by US Army under Contract: W911NF-04-C-0099.

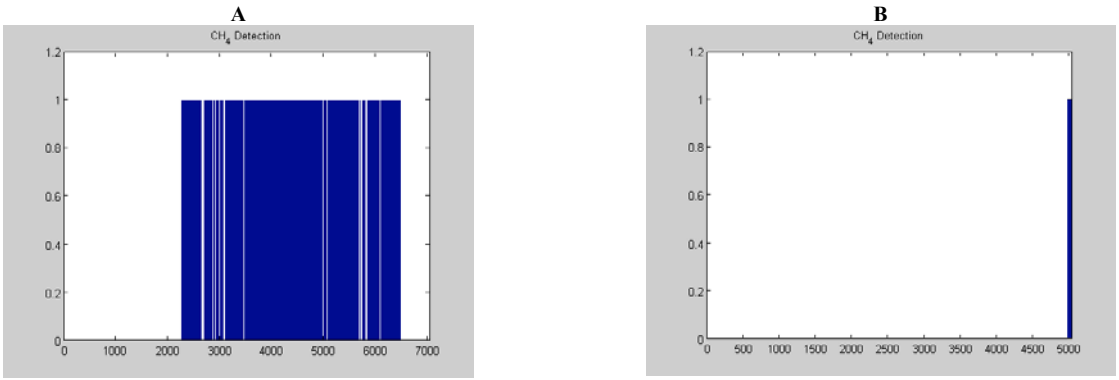

Figure 5-4: The detection results of the field experiments with the system shown in Figs. 5-1 – 5-2. A: results for the tube with methane, B: results for a free tube.

References

♦ Biswal, B. B., Ulmer, J. L. (1999) "*Blind Source Separation of Multiple Signal Sources of MRI Data Sets Using Independent Component Analysis*," J. Comput. Assist. Tomogr., 23, 265-271.

♦ Comon, P. (1994) "*Independent Component Analysis - a New Concept?*" Signal Processing 36, 287-314.

♦ Hahn, S.L. (1996), *Hilbert Transforms in Signal Processing*, Artech House, Norwood, Maryland, 1996.

♦ Hodgkinson, J., Pride, R. D. (2005), "*Gas Leak Imaging*", Business Briefing: Exploration & Production: The Oil & Gas Review, 2005, Issue 2.

♦ Hyvarinen, A. (1999), "*Survey on Independent Component Analysis*," Neural Computing Surveys, 2, 94-128.

♦ Hyvarinen, A., Oja, E. (1997) "*A Fast Fixed-point Algorithm for Independent Component Analysis*", Neural Computation, 9, 1483-1492.

♦ Jutten, C., Herault, H. (1991) "*Blind Separation of Sources, Part I: an Adaptive Algorithm Based on Neuromimatic Architecture*," Signal Processing, 23, 1-10.

♦ Long, S.R. (1995) "*The Hilbert Techniques: An Alternate Approach for Non-Steady Time Series Analysis*," IEEE Geoscience and Remote Sensing Society Newsletter, pp. 6-11, March 1995.

♦ O'Brien, J. J., Cao, H. (2002), "*Cross sections from Absorption Spectra and Absorption Coefficients for Methane in the 750-940 nm Region Obtained by Intracavity Laser Spectroscopy*," Journal of quantitative spectroscopy and radiative transfer 75, pp. 323-350.

♦ Park, H. M.; Jung, H. Y.; Lee, T. W.; Lee., S. Y. (1999), "*Subband-based Blind Signal Separation for Noisy Speech Recognition*," Electronics Lett., 35, 2011-2012.

♦ Platt, U. (1994) "*Differential optical absorption spectroscopy (DOAS)*,"in *Air Monitoring by Spectroscopic Techniques*, M. W. Sigrist, ed., Chemical Analysis Series (Wiley, New York), Vol.127.

♦ Tu, T.-M. (2000) "*Unsupervised signature extraction and separation in hyperspectral images: a noiseadjusted fast independent component analysis approach*," Optical Engineering, 39, pp. 897–906.

♦ Vigario, R. N. (1997) "*Extraction of Ocular Artifacts from EEG using Independent Component Analysis*," Electroencephalograph. Clin. Neurophysiol., 103, 395-404.

♦ Wu, H. T., J. F. Yang, and F. K. Chen (1995), ''*Source number estimation using transformed Gerschgorin radii*,'' IEEE Transactions on Signal Processing, 43, pp. 1325–1333.

♦ Ypma, A., Pajunen P. (1999) "*Rotating Machine Vibration Analysis with Second-order Independent Component Analysis*," Proc. Workshop on Independent Component Analysis and Signal Separation (ICA¢99); Aussois, France,; pp 37-42.